Analytical Methods

Accepted Manuscript

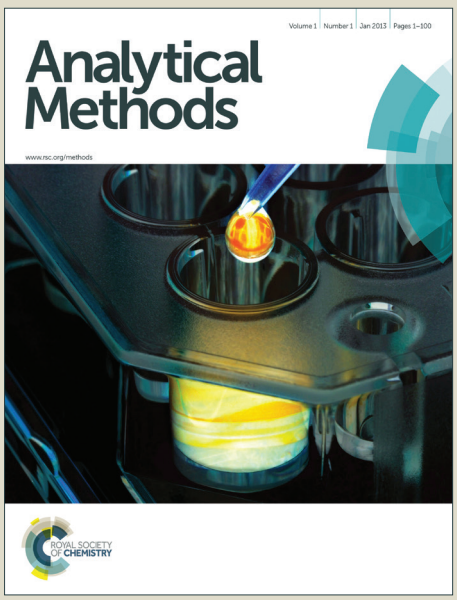

ROYAL SOCIETY OF CHEMISTRY

www.rsc.org/methods

Journal Name

RSCPublishing

ARTICLE

A sensitive impedimetric DNA biosensor for the determination of the HIV gene based on electrochemically reduced graphene oxide

Qiaojuan Gong*, Haiying Yang*, Yanyun Dong and Wenchan Zhang

Cite this: DOI: 10.1039/xOxxOOOOOx

Received OOth January 2012,
Accepted OOth January 2012

DOI: 10.1039/xOxxOOOOOx

www.rsc.org/

A sensitive impedimetric DNA biosensor for the determination of the HIV-1 gene was developed by employing electrochemically reduced graphene oxide (ERGO) as a sensing platform. The DNA biosensor was fabricated by drop-coating graphene oxide (GO) on a glassy carbon (GC) electrode and covalently immobilizing the designed single-stranded DNA (ssDNA) probe onto GO using carbodiimide chemistry. The GO was later electrochemically reduced to ERGO and applied to genosensing. Upon the occurrence of hybridisation events between the surface-confined ssDNA probe with the target DNA in solution to form a double-stranded DNA (dsDNA) at the electrode surface, the negative charge in the electrode/electrolyte interface, and as such, the electron transfer resistance of the electrodes toward the $[Fe(CN)_6]^{3-/4-}$ redox couple were changed. Such a change was used for impedimetric DNA biosensing. It was found that the employment of ERGO as immobilization platform could efficiently accelerated the electron transfer and enhance the EIS response of the DNA biosensor. Under the conditions employed in this study, the change of the electron transfer resistance was linear with the logarithm of the concentration of target DNA within a concentration range of 1.0×10^{-12} to 1.0×10^{-9} M with a detection limit of 3.0×10^{-13} M (S/N = 3). This strategy eliminated the requirement for DNA labelling, greatly simplifying the procedure. This work demonstrates that the employment of GO as an immobilization platform and ERGO as a biosensing platform is a promising approach to designing impedimetric aptasensors with high sensitivity and selectivity.

1. Instruction

The need for a sensitive method for the detection of DNA has attracted considerable attention due to its diverse applications including the identification of genetic diseases and disorders and the detection and characterization of genetic viruses, bacteria, and parasites.[1] Traditional methods for the detection of DNA on the basis of base-pair hybridization, such as gel electrophoresis or membrane blots, are slow and labour-intensive. DNA hybridization biosensors offer considerable promise for obtaining sequence-specific information in a simpler, faster and cheaper manner compared to traditional hybridization assays.[2] Various DNA biosensors have been established including fluorescence imaging,[3,4] optical,[5-7] electrochemical,[8-10] electrogenerated chemiluminescence (ECL) [11-13] and quartz crystal microbalance.[14] Although a DNA biosensor using an optical readout has many advantages such as high sensitivity, it needs much expensive instrumentation for optical imaging, laser light and labelled probes. Furthermore, the detection limit of the optical biosensor depends on the thickness of the test solution. Compared to an optical biosensor, an electrochemical biosensor has many advantages such as inexpensive instrumentation, low detection limit and simplicity due to the ease of obtaining an electrical signal.[15]

Extensive efforts have been devoted to designing an electrochemical DNA biosensor to improve the sensitivity and specificity, to reduce the cost and to simplify the fabrication steps. They include the employment of different electrode materials and electrode configurations, the development of efficient immobilization methods, the exploitation of novel redox probes and label-free strategies. Various nanomaterials have been employed as signal transducers on which nucleic acids are immobilized to improve the detection sensitivity. These substrates possess high surface area and good conductivity, providing more binding sites and surface-enhanced charge transfer for enhanced selectivity and sensitivity.[16] Nanomaterials combined with electrochemical biosensors are emerging options for DNA detection including gold nanoparticles,[17,18] polyaniline nanotubes,[19] silica-carbon nanofibers,[20] carbon nanotubes[21] and graphene.[22-25]

Graphene has attracted considerable attention owing to its extraordinary structure and electrical properties, tuneable surface functionalities and catalytic properties. Compared with graphene, graphene oxide (GO) is easily functionalized/decorated due to the presence of some oxygen-containing groups such as -COOH, -OH, and C=O groups at the edge of the graphene oxide sheet and the good dispersion of GO in aqueous solvents.[23] Given the ease of processing and handling GO and its electrochemical flexibility, it should come as no surprise that the recent efforts to produce approaches using GO resulted in a wide range of biosensing

applications such as DNA,[22-25] MicroRNA,[27] small molecule[28] and protein detection.[29] Liu et al.[30] reported a sensor for the detection of DNA by adsorption of a fluorophore-labelled DNA probe on GO. Hu et al.[22] developed a label-free electrochemical impedance spectroscopy (EIS) DNA biosensor for the detection of human immunodeficiency virus-1 (HIV-1) gene by GO anchored on a diazonium functionalized electrode, in which the immobilization of the DNA sequence was based on π-π stacking interactions. The DNA hybridization induced GO interfacial property changes and a conformation transition from 'lying' single-stranded DNA (ssDNA) to 'standing' double-stranded DNA (dsDNA), with a detection limit of 1.1×10^{-13} M. The attractive forces between DNA and GO include π–π stacking, hydrophobic interactions, hydrogen bonding, and van der Waals forces.[30] Without a covalent linkage, DNA adsorption is reversible. Bonanni et al.[24] developed an electrochemical assay for the detection of DNA by the covalent linking of ssDNA to GO using carbodiimide chemistry, and four different chemically modified graphenes for functionalization by ssDNA were thoroughly investigated. The results showed that DNA-graphene hybrid structures exhibit strong biorecognition ability and could be used for highly selective and sensitive detection of DNA. The incorporation of a signal molecule labelling step into the nucleic acid assay has the shortcomings of limited labelling efficiency, complex multi-step analysis and contamination of samples. The electrochemical reduction of GO (ERGO) has been proven to be a green and facile way to synthesize graphene films of high quality due to the intrinsic graphene structure. Moreover, the electrical conductivity of ERGO is approximately 8 orders of magnitude larger than that of the GO film.[31] This work employed ERGO as a supporting material to covalently anchor the ssDNA probe and developed an efficient method for increasing the sensitivity and preparing simple EIS biosensors.

The World Health Organization (WHO)/Joint United Nations Program on HIV/AIDS (UNAIDS) estimates that 40 million people are living with human immunodeficiency virus (HIV)/acquired immune deficiency syndrome (AIDS) infection to date.[32] The standard diagnostic tests for HIV infection are blood tests: enzyme immunoassay, enzyme-linked immunosorbent assay (ELISA), and Western blot test. All of these tests check for the presence of antibodies to HIV; they do not check for the virus itself. Compared to an immunoassay in which antibodies need a long period to be generated, genetic testing can operate in real-time once the patient is infected. Therefore, highly specific, rapid, and convenient HIV detection systems are required to facilitate the identification of infected individuals, preventing them from further infecting others, monitoring the disease progression of infected individuals, and investigating clinical trials of new drugs or vaccine candidates.[15, 33]

In this paper, we describe a simple, sensitive impedimetric DNA biosensor for the determination of the HIV-1 gene based on ERGO as a sensing platform. A HIV-1 gene (38-mer ssDNA from HIV-1 U5 long terminal repeat gene sequence)[34] was chosen as the target analyte. A schematic representation of the DNA biosensor with fabrication steps and performance is shown in Scheme 1. The DNA biosensor was designed by covalently immobilizing an amino-modified ssDNA probe onto the surface of a GO-modified glassy carbon (GC) electrode followed by electrochemically reduction to an ERGO/GC electrode. Upon the hybridization of the probe DNA with its complementary target DNA in solution, the electron transfer resistance for the negatively charged $[Fe(CN)_6]^{3-/4-}$ redox probe remarkably increased due to the enhanced electrostatic repulsion between the dsDNA duplex and $[Fe(CN)_6]^{3-/4-}$ redox probe. The increase in the electron transfer resistance could consequently be used as the readout of the biosensor. The introduction of ERGO as the electronic transducer on the DNA biosensor efficiently accelerated the electron transfer and enhanced the EIS response of the DNA biosensor. The fabrication and performance of the DNA biosensor was presented.

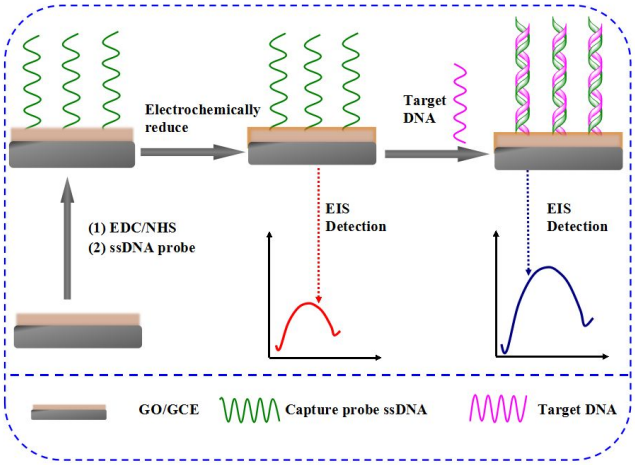

Fig. 1. Schematic diagram of the fabrication of the impedimetric DNA biosensor and the detection of target DNA.

2. Experimental

2.1 Materials and apparatus

A HIV-1 gene (38-mer ssDNA from HIV-1 U5 long terminal repeat gene sequence) was selected as the target DNA, 5'-GCT AGA GAT TTT CCA CAC TGA CTA AAA GGG TCT GAG GG-3'.[13, 34] A 20-mer 5'-CAG TGT GGA AAA TCT CTA GC-$(CH_2)_6$-NH_2-3' was used as the probe DNA. Two-base mismatch DNA (5'-GCT AGA GAT TGG CCA CAC TGA CTA AAA GGG TCT GAG GG-3') and non-complementary DNA (5'-CCT TTT AGT CAG TGT GGA AAA TCT CTA GCA GTG GC-3') were used to investigate the selectivity of the DNA biosensor. All oligonucleotides used were purchased from Sangon Bioengineering Ltd. Co. (Shanghai, China). All oligonucleotide stock solutions (0.1 mM) were prepared with 10 mM tris-HCl solution (pH 7.40, 1 mM EDTA) and stored at -20 °C. 10 mM phosphate buffer saline (PBS, pH 7.40, 0.10 M NaH_2PO_4/Na_2HPO_4 and 0.10 M KCl) was used as the hybridization buffer and washing solution.

Graphite powder (320 mesh) was spectroscopically pure and obtained from Shanghai Chemicals (Shanghai, China). N-(3-dimethylaminopropy)-N'-ethylcarbodiimide hydrochloride (EDC), N-hydroxysuccinimide (NHS) and tris(hydroxymethyl)-aminomethane were purchased from Sigma-Aldrich (USA). Methylene blue (MB) was obtained from Xi'an Chemical Reagent Company (Xi'an, China). Alumina powder (0.3 μm) was purchased from Buehler (USA). All reagents were of analytical grade and used as received. All aqueous solutions were prepared with ultra-pure water (18 MΩ·cm) from a Milli-Q Plus system (Millipore).

A CHI 660 electrochemical workstation (Chenhua Instruments Co., Shanghai, China) was used for the electrochemical measurements. All experiments were carried out using a conventional three-electrode system with a fabricated DNA sensor or a glassy carbon (GC) electrode (diameter 3.0 mm) as the working electrode, a platinum wire as the counter electrode and an Ag/AgCl (sat. KCl) as the reference electrode. All potentials are relative to this reference electrode. Fourier transform infrared (FT-IR) spectra

were recorded on a KBr disk using a Tensor 27 FT-IR Spectrometer (Bruker, Germany). Scanning electron microscopic (SEM) images were obtained with a Hitachi S-4800 (Japan). Transmission electron micrographs (TEM) were obtained on a JEM-2100 TEM (JEOL, Japan). Raman spectra were obtained with an inVia Raman Microscope (Renishaw, British).

2.2 Fabrication of the DNA biosensor and hybridization

Graphene oxide was prepared from natural graphite powder by a modified Hummer's method.[35] The as-synthesized graphite oxide was suspended in water and subjected to dialysis for one week to remove residual salts. After drying at 50 °C overnight, as purified graphite oxide was exfoliated into GO by ultrasonicating a 0.05 wt% aqueous dispersion for 30 min. Unexfoliated graphite oxide was removed by a ultrafiltration at 2000 rcf for 5 min.

The GC electrode was polished with 0.3 μm alumina slurry and then ultra-sonicated in water for 5 min. 2.0 mg GO was ultrasonically dispersed in 10 mL of water. 5 μL of the dispersed GO suspension was drop-coated onto the surface of the pretreated GC electrode and dried in air. The GO/GC electrode was washed with 10 mM PBS and activated in 0.1 mL of freshly prepared solution containing 2 g L^{-1} EDC and 5 g L^{-1} NHS for 30 min and then was washed with 10 mM PBS. 10 μL of 0.01 μM capture probe was coated on the activated GO/GC electrode for 1 h at 25 °C. 10 μL of 10 mM PBS containing 1 mM ethanolamine was dropped onto the surface of capture probe modified GO/GC electrode and maintained for 15 min to deactivate the remaining succinimide groups and to block unreacted active sites on the surface of the electrode.[36] After washing with DNA buffer, the capture probe modified GO/GC electrode was electrochemically reduced by cyclic voltammetry in 10 mM PBS from -1.7 ~ 0.0 V with scan parameters of 100 mv s^{-1}, 50 circles.[37] Finally, the obtained biosensor was washed with DNA buffer and stored at 4 °C before use.

The DNA hybridization reaction was conducted by dropping 5 μL of a fixed concentration of target HIV-1 gene solution onto the DNA sensor surface and allowing it to react for 1 h. Then, the electrode was rinsed with DNA buffer solution to remove unhybridised DNA. The same procedure as mentioned above was applied to hybridization with mismatched DNA sequences.

2.3 Electrochemical measurement

After the hybridization reaction, the sensor was placed into an electrochemical cell containing 5 mL of 10 mM PBS (pH 7.40), 5.0 mM $K_4[Fe(CN)_6]/K_3[Fe(CN)_6]$ and 0.10 M KCl. Electrochemical impedance spectroscopy (EIS) was taken, in which the open circuit potential was used as a DC bias potential on which the amplitude of the AC potential was 5 mV. The EIS was recorded over the frequency from 100 kHz to 0.1Hz with a sampling rate of 12 points per decade. 2 s of quiet time was allowed before each measurement. The concentration of HIV-1 was quantified by an increase of the electron transfer resistance ΔR_{et} ($\Delta R_{et} = R_{et,\,i} - R_{et,0}$), where $R_{et,0}$ is the electron transfer resistance in the absence of HIV-1 and $R_{et,\,i}$ is the electron transfer resistance in the presence of HIV-1. The cyclic voltammogram signals of the accumulated methylene blue (MB) were obtained in 10 mM PBS (pH 7.40) containing 20 μM MB. Working electrodes were transferred into the MB solution and accumulated for 10 min. Then, they were rinsed and placed in MB-free PBS buffer, where the cyclic voltammogram was performed with a potential range of + 0.15 V to − 0.40 V. All electrochemical experiments were carried out at room temperature (25±1 °C).

3. Results and Discussion

3.1 Characterization of GO and the fabrication of the DNA biosensor

Fig. 2 shows the FT-IR spectrum, Raman spectrum and TEM of GO to illustrate its structure and morphology. The FT-IR spectrum of GO displays the characteristic bands of a carboxylic group (C=O stretching at *ca*. 1737 cm^{-1}), an epoxy group (C=O vibration at *ca*. 1095 cm^{-1}), a hydroxyl group (O-H vibration at *ca*. 3236 cm^{-1}), and C=C bonds (C=C stretching at *ca*. 1614 cm^{-1}) (Fig. 2A), and the results were in accordance with the literature.[34] These confirm the successful oxidation of graphite due to the abundance of hydrophilic groups, i.e., -OH, -COOH and epoxides, on the surface of the obtained GO, which is favourable to the building of the nano/bio interface. Fig. 2B shows the Raman spectra of graphite and GO, respectively. The typical features in the Raman spectra of carbonaceous materials are the D band at ~1365 cm^{-1}, which is attributed to local defects and disorders, particularly the defects located at the edges of graphite platelets, and the G band at ~1596 cm^{-1}, which is generally assigned to the E_{2g} phonon of sp^2 bonds of carbon atoms.[38] The graphite shows a small D peak at 1356 cm^{-1} and a strong G peak at 1565 cm^{-1}(Fig. 2B, curve a). As for GO (Figure 2B, curve b), the spectrum shows broad D and G peaks at 1356 cm^{-1} and 1606 cm^{-1}, respectively, which are in accordance with the reference.[38] The TEM analysis of GO is shown in Fig. 2C. The characteristic morphology of GO can be observed from the image, displaying the featureless basal plane across the majority of the region and the folded sheets at certain locations. Meanwhile, structures with mostly smooth basal planes and sharp edges were also observed. The morphology of the ERGO/GC electrode was also examined by SEM. As shown in Fig. 2 D and E, ERGO films dispersed on the GC electrode surface exhibited a curly morphology consisting of a thin wrinkling paper-like structure, which is in agreement with the chemical reduction of GO on the GC electrode surface.[31] After the ssDNA probe is immobilized on the ERGO/GC electrode, some small particles were observed on the crumpled and wrinkled structures of graphene, which might be the ssDNA immobilized on the surface.

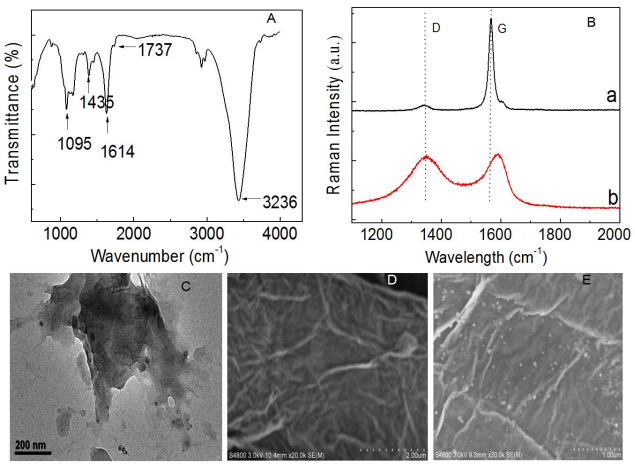

Fig. 2. FT-IR spectrum (A), Raman spectrum (B), and TEM image (C) of GO; SEM images of GO/GC electrode (D) and ssDNA/ERGO/GC electrode (E). Raman spectrum of GO was obtained by laser excitation at a wavelength of 532 nm.

Electrochemical impedance spectroscopy (EIS) has proven to be one of the most powerful tools for determining the characteristics of interfacial properties in the biosensor fabrication process and binding process.[15] Nyquist plots of the GC electrode subjected to the step-by-step modification process, using $[Fe(CN)_6]^{4-/3-}$ as the redox indicator, were generated. As shown in Fig. 3A (inset), the Randles equivalent circuit [39] was found to fit adequately the data obtained over the measured frequency range, which includes electron transfer resistance (R_{et}), electrode/electrolyte solution (R_s) and the Warburg impedance (Z_w). The two elements of the Randles equivalent circuit, R_s and Z_w, represent the properties of the bulk solution and the diffusion of the redox probe, and they are not affected by the reaction occurring at the electrode surface. The other two elements, C_{dl} and R_{et}, depend on the dielectric and insulating features at the electrode/electrolyte interface. Among these electrical parameters, we focused on the R_{et} value recorded after each modification step because the electron transfer process of $[Fe(CN)_6]^{4-/3-}$ is strongly influenced by electrode modification. From Fig. 3A, it can be observed that the bare GC electrode exhibits a very small semicircle at high frequencies, and the R_{et} was 255 Ω. The GO-coated GC electrode resulted in an increase in R_{et} from 255 Ω to 8657 Ω, which was in agreement with the results obtained from the study of DNA probes immobilized onto graphene-based electrode surfaces.[23, 24] When GO was modified onto the GC electrode surface, the R_{et} value increased relative to the bare GC electrode, suggesting that GO acted as an insulating layer that hindered the interfacial electron transfer due to its disrupted sp^2 bonding networks.[40] When the ssDNA probe was covalently immobilized onto the GO/GC electrode, the R_{et} increased to 62310 Ω. This is attributed to the fact that the immobilized ssDNA with a single strand nucleic acid with negative charges on its phosphate backbone has an electrostatic repulsive force to $[Fe(CN)_6]^{4-/3-}$. This indicates that the ssDNA probe has been assembled onto the surface of the GO/GC electrode. The surfaces were then electrochemically reduced by scanning from 0.0 to -1.7 V, and the R_{et} sharply decreased to 4839 Ω, which indicates a reduction in GO (the electrode surface is now referred to as the ssDNA/ERGO/GC electrode). After the electrochemical reduction of GO, the electrochemical behaviour of the electrode toward the redox probe improved significantly because of the high conductivity and the neutral nature of the ERGO sheets.[41] It was found that the employment of ERGO as immobilization platform could efficiently accelerated the electron transfer and enhance the EIS response of the DNA biosensor. After the target DNA (HIV-1) was hybridized, the R_{et} increased to 20980 Ω. When the probe sequence in ssDNA was hybridized with its target DNA sequence, the double-helix structure between the probe and target formed. Hybridization brought more negatively charged phosphate backbones, which prevented the $[Fe(CN)_6]^{4-/3-}$ from penetrating the double-helix bundles. Hence, the R_{et} value increased with dsDNA formation, and an impedimetric signal-on process was achieved. The results suggest that the DNA biosensor was successfully fabricated and could detect the target HIV-1 successfully

Cyclic voltammetry experiments with the same electrode systems were further used to investigate the changes of the electrode behaviour after each assembly step (Fig. 3B), and the results were in agreement with the findings from the EIS work. It is well known that many of the methods used to produce GO introduce defects, functional groups, carbonaceous impurities and metallic impurities into the GO structure that are difficult to remove. Impurities at edge planes, particularly pervasive oxygen-containing functional groups, can be beneficial for electrochemistry, as these are likely to be major sites for rapid heterogeneous electron transfer. However, rapid electron transfer is of little use without a reasonable rate of charge transport within the GO to move the electrons to or from the supporting electrode, so there should be an optimal balance between the levels of oxidation and reduction that can give a reasonable number of functional groups and defects for electron-transfer reactions while maintaining an appropriately high level of conductivity.[38]

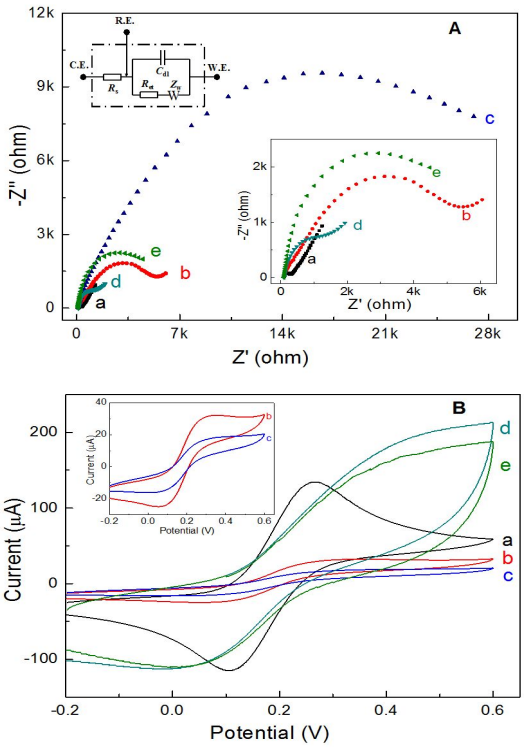

Fig. 3. Nyquist plots of the impedance spectra (A) and cyclic voltammograms (B) of different electrodes in each step of the fabrication of the DNA biosensor and the determination of the HIV-1 gene in a solution of 10 mM PBS (pH 7.40) containing 5 mM $K_3Fe(CN)_6$–5 mM $K_4Fe(CN)_6$–0.10 M KCl. Curve a, bare GC electrode; curve b, GO/GC electrode; curve c, ssDNA/GO/GC electrode; curve d, ssDNA/ERGO/GC electrode; curve e, ssDNA/ERGO/GC electrode after incubation with HIV-1 gene for 60 min. Inset: (A) Randles equivalent circuit used to model the impedance data in the presence of the redox couple (left hand corner); enlarged Nyquist plots of a, b, d and e (right hand corner); (B) enlarged cyclic voltammograms of b and c (left hand corner).

3.2 Electrochemical characteristics of the DNA biosensor

DNA nucleobases could be directly oxidized at the electrode surface with the oxidation potential increasing in the order of G < A < T < C. In this case, the direct electrochemistry of ssDNA immobilized on an electrochemically reduced GO-modified electrode was also examined. Two well-defined peaks were observed at 1.019 V and 1.219 V (Fig. 4A), corresponding to the electrochemical oxidation of the A and T bases, respectively. The results were in accordance with previous reports that a single nucleotide polymorphism detection could be achieved at a chemically reduced GO-modified electrode.[31] These results demonstrate that the large surface area and unique structure of ERGO provide good candidates for ssDNA grafting.

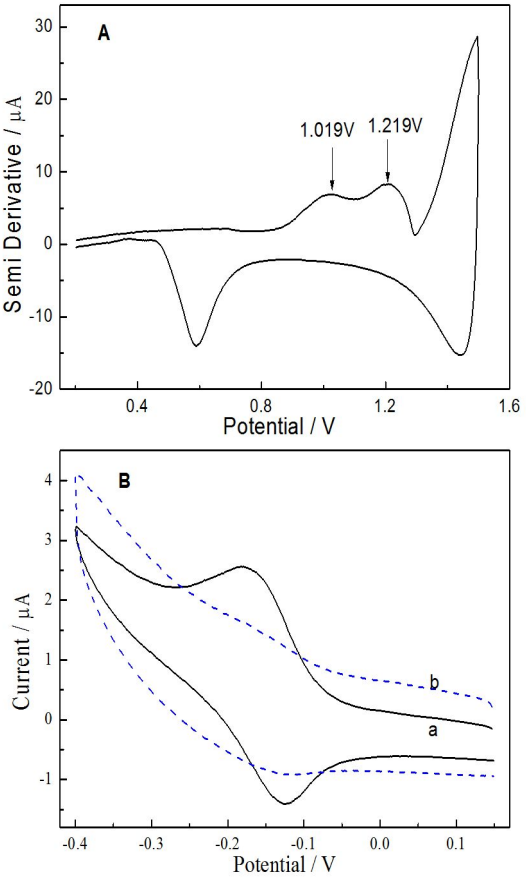

Fig. 4. (A) Cyclic voltammograms of ssDNA/ERGO/GC electrode. (B) Cyclic voltammograms of adsorbed MB at the ssDNA/GO/GC electrode (a) and ssDNA/ERGO/GC electrode (b) in MB-free PBS solution (pH 7.40) at a scan rate of 100 mv s^{-1}.

To confirm electrode modification and further illustrate ssDNA immobilization, the electrochemical behaviour of MB at the GO/GC electrode and the ERGO/GC electrode was checked (Fig. 4B). MB could be intercalated into the DNA chain, giving rise to different electrochemical characteristics compared to its interaction at normal surfaces. MB, a positively charged aromatic heterocycle belonging to the phenothiazinyl family, has been reported to adsorb to a graphitic surface through π-stacking, charge-transfer and hydrophobic interactions[22, 42] and to interact with ssDNA through electrostatic interactions and specific binding with guanine residues.[42] After immersion in the MB solution for 10 min, the electrodes, namely the ssDNA-immobilized GO/GC electrode and ERGO/GC electrode, were placed in MB-free PBS solution to perform potential cycling. As shown in Fig. 4B, at the ssDNA/GO/GC electrode, a pair of recognizable redox peaks with high current intensities was observed (curve a) due to the π-stacking adsorption of MB on the GO sheet and the electrostatic attraction of MB on the phosphate backbones of ssDNA. This is the two electron and one proton transfer oxidation/reduction process between MB and the reduced form as leucomethylene blue (LB).[43] The ssDNA probe was immobilized on the GO platform according to covalent interactions, and its negatively charged phosphate backbones were exposed. Consequently, the dominating electrostatic attraction took place to attract positively charged MB. While at the ssDNA immobilized ERGO/GC electrode (curve b), MB/LB redox peak currents obviously decreased. This may be attributed to the removal of a considerable number of oxide groups from GO, which resulted in the decrease of the amount of adsorbed MB.[22] Comparing with the adsorption of MB on the ssDNA/GO/GC electrode, the low amount of electrostatically attracted MB contributed to the low peak currents.

3.3 Optimization of the capture probe concentration for immobilization

The concentration of the capture probe for the fabrication of the biosensor directly influences the surface coverage of the ssDNA probe on the ERGO/GC electrode for HIV-1 detection. Fig. 5 shows the dependence of the R_{et} value on the ssDNA concentration when incubated with 1.0×10^{-11} M HIV-1. From Fig. 5, it can be observed that the R_{et} value increases with an increase of the capture probe concentration from 1.0×10^{-10} M to 1.0×10^{-8} M due to the increase of the surface coverage of the ssDNA probe. Then, the R_{et} value decreases with the increase of the ssDNA probe concentration from 1.0×10^{-8} M to 1.0×10^{-4} M, which may be related to the fact that the high-concentration probes might weaken the density of the capture probes on the electrode surface or the high-concentration probes might increase the steric hindrance of the microenvironment. Therefore, a 1.0×10^{-8} M capture probe was used to obtain a high sensitivity.

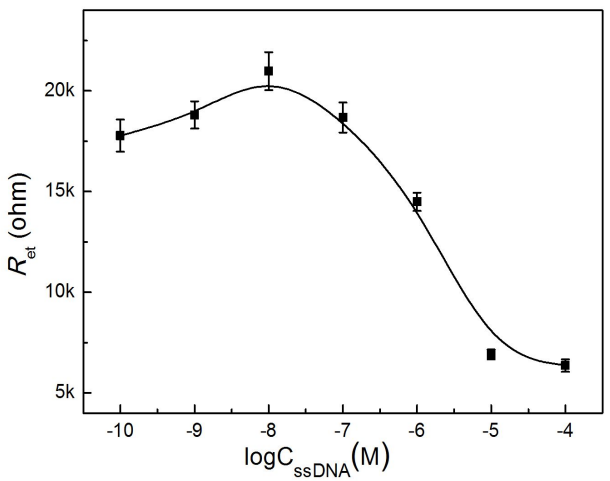

Fig. 5. Dependence of the R_{et} on the concentration of the capture probe ssDNA. The biosensors were incubated with 1.0×10^{-11} M HIV-1 gene for 60 min. EIS measurement conditions were the same as in Fig. 3.

3.4 Performance of the DNA biosensor for HIV-1

The quantitative behaviour of the DNA biosensor was assessed by measuring the dependence of ΔR_{et} on the concentration of the HIV-1 gene under optimized conditions. Fig. 6A shows Nyquist plots of the faradic impedance spectra for the biosensor with different concentrations of the target HIV-1 gene (1.0×10^{-12} M ~ 1.0×10^{-9} M). The inset of Fig. 6A shows the logarithmic relationship between ΔR_{et} and the concentration of the HIV-1 gene. The regression equation was $\Delta R_{et} = 15945 \log C + 75728$ (C is in units of M) with a regression coefficient of 0.9936. The detection limit was estimated to be 3.0×10^{-13} M HIV-1 gene (S/N = 3[44, 45, 46]). A comparison of

this method with some reported genosensors in terms of the detection limit and the signal amplification strategy is provided in Table 1. The detection limit obtained is comparable to the 5.0×10^{-13} M obtained from a DNA impedimetric biosensor[23] and the 1.1×10^{-13} M obtained from an impedimetric genosensor using a diazonium-functionalized GO-modified electrode.[22] It is higher than that of the genosensors using gold nanorod decorated graphene oxide sheets,[25] supersandwiches[13] and bioconjugated nanoparticle amplification.[7] Although the detection limit obtained by differential pulse voltammetry with a gold nanorod decorated graphene oxide sheet is quite lower than that obtained in our work, it requires a complicated decorating procedure.[25] Therefore, the detection limit obtained here is considerably satisfactory. Based on the reported work in coupling polymer-based membrane[47-54] or nanomaterials,[55-58] significantly enhanced sensitivity may be achievable.

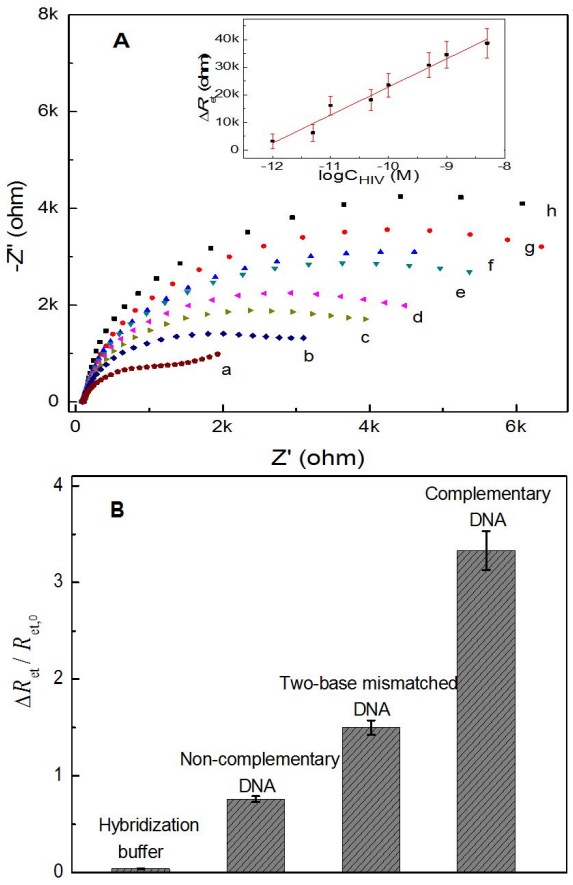

Fig. 6. (A) Nyquist plots of impedance spectra of the DNA biosensor for different concentrations of HIV-1 gene for 60min: (a) 0; (b) 1.0×10^{-12}; (c) 5.0×10^{-12}; (d) 1.0×10^{-11}; (e) 5.0×10^{-11}; (f) 1.0×10^{-10}; (g) 5.0×10^{-10}; and (h) 1.0×10^{-9} M. Inset: Dependence of ΔR_{et} on the logarithm of the concentration of HIV-1 gene. (B) The ΔR_{et} obtained with the DNA biosensors after the electrodes were incubated with target-free hybridization buffer, non-complementary DNA, two-base mismatched DNA and complementary DNA for 60 min. The concentration of the DNA sequences was 1.0×10^{-11} M. The illustrated error bars represent the standard deviations of three repeated measurements. EIS measurement conditions were the same as in Fig. 3.

The reproducibility of the DNA biosensor was estimated for the detection of 1.0×10^{-11} M target HIV-1 gene. The relative standard deviation obtained was 4.7 % using five individual biosensors and was 4.2 % for seven independent measurements using the same biosensor. This indicates that the reproducibility of the fabricated biosensor is feasible. The storage stability of the DNA biosensor was also examined. After storage at 4°C in 10 mM PBS (pH 7.40) for one week, the biosensor showed an average EIS value that was 95.6 % of initial EIS value for 1.0×10^{-11} M HIV-1 gene.

Table 1 Comparison of the proposed method with some reported genosensors

Detection technique/[a]	Detection Limit (M)	Signal amplification strategy	Reference
EIS	1.0×10^{-13}	Label-free ERGO-modified electrode	This work
EIS	1.1×10^{-13}	GO anchored on a diazonium-functionalized electrode	[22]
EIS	1.7×10^{-9}	Supersandwich	[10]
EIS	5.0×10^{-13}	3,4,9,10-perylene tetracarboxylic acid functionalized graphene-modified electrode	[23]
EIS	2.5×10^{-10}	Modified printed carbon electrodes	[24]
DPV	3.5×10^{-15}	Gold nanorod decorated graphene oxide sheet	[25]
SWV	1.0×10^{-10}	Methylene blue as a hybridization redox indicator	[15]
Fluorescence	8.0×10^{-16}	Bioconjugated nanoparticles	[7]
Fluorescence	4.0×10^{-11}	FAM-labelled GO/polymer complex	[59]
Chemiluminescence	6.5×10^{-10}	GO as chemiluminescence quencher	[60]
ECL	2.2×10^{-14}	Supersandwich	[13]
ECL	5.0×10^{-12}	Gold nanoparticle-modified electrodes	[11]

a ECL: electrogenerated chemiluminescence; ASV: anodic stripping voltammetry; SWV: square wave voltammetry; DPV: differential pulse voltammetry.

We also investigated the responses of the impedimetric DNA biosensors by incubating the ssDNA/ERGO/GC electrodes in target-free hybridization buffer and hybridization buffers containing different DNA sequences including non-complementary DNA and two-base mismatched DNA under optimized conditions. The results are shown in Fig. 6B. A negligible ΔR_{et} value was observed after the ssDNA/ERGO/GC electrodes were incubated in the target-free hybridization buffer, implying that the fabricated biosensor was stable under the present conditions. The increased EIS value ($\Delta R_{et}/R_{et}$) was 3.3 for the perfect-matched HIV-1 gene. In stark contrast, the increased EIS value was only 0.76 for non-complementary DNA and 1.5 for two-base mismatched HIV-1 gene. The values were smaller than that observed with complementary DNA, allowing discrimination of mismatched sequences. The increased R_{et} value was due to less efficient hybridization, attributed

to the mismatched bases in the sequence.[22] The ΔR_{et} values were to be 45.0% and 22.8% of that of hybridization with complementary DNA for two-base mismatched and non-complementary sequences. The results were in accordance with that obtained from an ECL DNA biosensor for the detection of the HIV-1 gene with a supersandwich ds-DNA structure and a ruthenium complex as an intercalated signal-producing compound.[13] In principle, hybridization with fully complementary sequences induced much greater interfacial property changes compared to with mismatched sequences due to the higher hybridization efficiency.[22] Hence, the largest ΔR_{et} value was observed after hybridization with complementary sequences in the present study. More mismatched bases exhibited greater interference with hybridization efficiency, resulting in less double helix formation and a lower signal intensity.

4. Conclusion

By taking advantage of GO with abundant oxygen-containing functional groups to immobilize the ssDNA probe and the good electrochemical properties of ERGO, we have developed an impedimetric DNA biosensor for the detection of the HIV-1 gene. It was found that the employment of ERGO as immobilization platform could efficiently accelerated the electron transfer and enhance the EIS response of the DNA biosensor. The ssDNA/ERGO-based DNA biosensor was sensitive and selective for the target DNA with a low detection limit down to 0.3 pM. And a good discrimination of mismatched or non-complementary sequence was also observed. Compared with the existing methods for DNA detection, the strategy eliminated the requirement for DNA labelling, representing a comparatively simple method. This method may also hold promise for potential applications in DNA biosensing and DNA nanostructure framework construction.

.

Acknowledgments

Financial support from the Science Foundation of Shanxi (no. 2012011007-1), the Technology Innovation Program of the Deparment of Education of Shanxi (no. 2013151), the Science Foundation of Bureau of Science and Technology of Yuncheng (no. 2060499) and the Scientific Research Foundation of Yuncheng University (no. YKU2014015, CY-2014006) are gratefully acknowledged.

Notes and references

Department of Applied Chemistry, Yuncheng University, Yuncheng, 044000, China.
Fax: +86 359 2090378; Tel: +86 359 8594394;
E-mail: hyyang@ycu.edu.cn; gqjuan@163.com.

1 E. G. Hvastkovs and D. A. Buttry, *Anal. Chem*., 2007, **79**, 6922–6926.
2 J. Wang, *Anal. Chim. Acta*, 2002, **469**, 63–71.
3 V. Benoit, A. Steel, M. Torres, Y. Y. Yu, H. Yang and J. Cooper, *Anal. Chem.*, 2001, **73**, 2412–2420.
4 Y. Dharmadi and R. Gonzalez, *Biotechnol. Progr*., 2004, **20**, 1309–1324.
5 Ahn and D. R. Walt, *Anal. Chem.*, 2005, **77**, 5041–5047.
6 T. A. Taton, G. Lu and C. A. Mirkin, *J. Am. Chem. Soc*., 2001, **123**, 5164–5165.
7 X. Zhao, R. T. Dytioco and W. Tan, *J. Am. Chem. Soc.*, 2003, **125**, 11474–11475.
8 R. Gasparac, B. J. Taft, M. A. Lapierre-Devlin, A. D. Lazareck, J. M. Xu and S. O. Kelley, *J. Am. Chem. Soc*., 2004, **126**, 12270–12271.
9 J. Wang, M. Musameh and Y. Lin, *J. Am. Chem. Soc*., 2003, **125**, 2408-2409.
10 L. Y. Zhou, X. Y. Zhang, G. L. Wang, X. X. Jiao, H. Q. Luo and N. B. Li, *Analyst*, 2012, **137**, 5071–5075.
11 H. Wang, C. Zhang, Y. Li and H. Qi, *Anal. Chim. Acta*, 2006, **575**, 205–211.
12 X. H. Xu, H. C. Yang, T. E. Mallouk and A. J. Bard, *J. Am. Chem. Soc*., 1994, **116**, 8386–8387.
13 S. Ruan, Z. Li, H. Qi, Q. Gao and C. Zhang, *Microchimica Acta*, 2014, **181**, 1293–1300.
14 X. Su, R. Robelek, Y. Wu, G. Wang and W. Knoll, *Anal. Chem.*, 2003, **76**, 489–494.
15 D. Zhang, Y. Peng, H. Qi, Q. Gao and C. Zhang, *Biosens. Bioelectron.*, 2010, **25**, 1088–1094.
16 C. P. Chen, A. Ganguly, C.H. Wang, C.W. Hsu, S. Chattopadhyay, Y.K. Hsu, Y.C. Chang, K. H. Chen and L. C. Chen, *Anal. Chem.,* 2008, **81**, 36–42.
17 C. Wang, X. Yuan, X. Liu, Q. Gao, H. Qi and C. Zhang, *Anal. Chim. Acta*, 2013, **799**, 36–43.
18 W. Wang, L. Song, Q. Gao, H. Qi and C. Zhang, *Electrochem. Commun.,* 2013, **34**, 18–21.
19 H. Chang, Y. Yuan, N. Shi and Y. Guan, *Anal. Chem*., 2007, **79**, 5111–5115.
20 V. Vamvakaki, M. Hatzimarinaki and N. Chaniotakis, *Anal. Chem.*, 2008, **80**, 5970–5975.
21 J. C. Claussen, A. D. Franklin, A. ul Haque, D. M. Porterfield and T. S. Fisher, *ACS Nano*, 2009, **3**, 37–44.
22 Y. Hu, F. Li, D. Han, T. Wu, Q. Zhang, L. Niu and Y. Bao, *Anal. Chim. Acta*, 2012, **753**, 82–89.
23 Y. Hu, F. Li, X. Bai, D. Li, S. Hua, K. Wang and L. Niu, C*hem. Commun*., 2011, **47**, 1743–1745.
24 Bonanni, A. Ambrosi and M. Pumera, *Chem.–Eur. J.*, 2012, **18**, 1668–1673.
25 X. Han, X. Fang, A. Shi, J. Wang and Y. Zhang, *Anal. Biochem*., 2013, **443**, 117–123.
26 L. Gao, C. Lian, Y. Zhou, L. Yan, Q. Li, C. Zhang, L. Chen and K. Chen, *Biosens. Bioelectron.*, 2014, **60**, 22–29.
27 H. Yin, Y. Zhou, H. Zhang, X. Meng and S. Ai, *Biosens. Bioelectron.*, 2012, **33**, 247–253.
28 Y. He, Z. G. Wang, H. W. Tang and D. W. Pang, *Biosens. Bioelectron.*, 2011, **29**, 76–81.
29 M. J. A. Shiddiky, S. Rauf, P. H. Kithva and M. Trau, *Biosens. Bioelectron.*, 2012, **35**, 251–257.
30 B. Liu, Z. Sun, X. Zhang and J. Liu, *Anal. Chem*., 2013, **85**, 7987–7993.
31 M. Zhou, Y. Zhai and S. Dong, *Anal. Chem.*, 2009, **81**, 5603-5613.
32 J. McMichael, *Annu. Rev. Immunol.*, 2006, **24**, 227–255.
33 C. Kim, M. K. Ju, A. D. Chin Yu and P. Sommer, *Anal. Chem.*, 2009, **81**, 2388–2393.
34 X. Chen, C. Y. Hong, Y. H. Lin, J. H. Chen, G. N. Chen and H. H. Yang, *Anal. Chem.*, 2012, **84**, 8277–8283.
35 Y. Li and Y. Wu, *J. Am. Chem. Soc.*, 2009, **131**, 5851–5857.

36 E. Radi, X. Muñoz-Berbel, V. Lates and J. L. Marty, *Biosens. Bioelectron.*, 2009, **24**, 1888–1892.
37 S. N. Prashanth, N. L. Teradal, J. Seetharamappa and A. K. Satpati, *J. Electrochem. Soc*., 2014, **161**, B117–B122.
38 K. R. Ratinac, W. Yang, J. J. Gooding, P. Thordarson and F. Braeta, *Electroanalysis*, 2014, **26**, 139–146.
39 F. Patolsky, M. Zayats, E. Katz and I. Willner, *Anal. Chem.*, 1999, **71**, 3171–3180.
40 D. R. Dreyer, S. Park, C. W. Bielawski and R. S. Ruoff, *Chem. Soc. Rev.,* 2010, **39**, 228–240.
41 M. J. Haque, H. Park, D. Sung, S. Jon, S. Y. Choi and K. Kim, *Anal. Chem*., 2012, **84**, 1871–1878.
42 Y. Yan, M. Zhang, K. Gong, L. Su, Z. Guo and L. Mao, *Chem. Mater*., 2005, **17**, 3457–3463.
43 E. Farjami, L. Clima, K. V. Gothelf and E. E. Ferapontova, *Analyst*, 2010, **135**, 1443–1448.
44 R. N. Goyal, V. K. Gupta and N. Bachheti, *Anal. Chim. Acta*, 2007, **597**, 82–89.
45 R. N. Goyal, V. K. Gupta and S. Chatterjee, *Talanta*, 2008, **76**, 662–668.
46 L.A. Currie, *Pure &Appl. Chem.*, 1995, **67,** 1699–1723.
47 R. N. Goyal, V. K. Gupta and S. Chatterjee, *Electrochim. Acta*, 2008, **53**, 5354–5360.
48 V. K. Gupta, A. K. Singh, M. A. Khayat and B. Gupta, *Anal. Chim. Acta*, 2007, **590**, 81–90.
49 V. K. Gupta, R. Mangla, U. Khurana and P. Kumar, *Electroanalysis*, 1999, **11**, 573–576.
50 V. K. Gupta, S. Jain and U. Khurana, *Electroanalysis*, 1997, **9**, 478–480
51 V. K. Gupta, R. Prasad, P. Kumar and R. Mangla, *Anal. Chim. Acta*, 2000, **420**, 19–27.
52 R. Prasad, V. K. Gupta and A. Kumar, *Anal. Chim. Acta*, 2004, **508**, 61–70.
53 V. K. Gupta, A. Nayak, S. Agarwal and B. Singhal, *Comb. Chem. High Throughput Screen*., 2011, **14**, 284–302.
54 R. Jain, V. K. Gupta, N. Jadona and K. Radhapyari, *Anal. Biochem*., 2010, **407**, 79–88.
55 V. K. Gupta, R. Jain, K. Radhapyari, N. Jadon and S. Agarwal, *Anal. Biochem*., 2011, **408**, 179–196.
56 V. K. Gupta, M. R. Ganjali, P. Norouzi, H. Khani, A. Nayak and S. Agarwal, *Crit. Rev. Anal. Chem*., 2011, **41**, 282–313.
57 P. Norouzi, V. K.Gupta, F. Faridbod, M. Pirali-Hamedani, B. Larijani and M. R. Ganjali, *Anal. Chem.*, 2011, **83**, 1564–1570.
58 P. Norouzi, V. K. Gupta, B. Larijani, S. Rasoolipour, F. Faridbod and M. R. Ganjali, *Talanta*, 2015, **131**, 577–584.
59 X. J. Xing, X. G. Liu, Y. He, Y. Lin, C. L. Zhang, H. W. Tang and D. W. Pang, *Biomacromolecules*, 2013, **14**, 117–123.
60 Y. He, G. M. Huang and H. Cui, *ACS Appl. Mater. Interfaces*, 2013, **5**, 11336–11340.

A table of contents of entry (Manuscript ID AY-ART-01-2015-000111)

Text:

A sensitive impedimetric DNA biosensor for the determination of the HIV gene was developed by employing electrochemically reduced graphene oxide as a sensing platform.

Colour graphic: